JVI Journals.ASM.org

Differential Contributions of Tacaribe Arenavirus Nucleoprotein N-Terminal and C-Terminal Residues to Nucleocapsid Functional Activity

Alejandra D'Antuono,[a] Maria Eugenia Loureiro,[a]* Sabrina Foscaldi,[a] Cristina Marino-Buslje,[b] Nora Lopez[a]

Centro de Virología Animal (CEVAN), Instituto de Ciencia y Tecnología Dr. Cesar Milstein, Consejo Nacional de Ciencia y Tecnología (CONICET), Ciudad Autónoma de Buenos Aires, Argentina[a]; Fundación Instituto Leloir, Ciudad Autónoma de Buenos Aires, Argentina[b]

ABSTRACT

The arenavirus nucleoprotein (NP) is the main protein component of viral nucleocapsids and is strictly required for viral genome replication mediated by the L polymerase. Homo-oligomerization of NP is presumed to play an important role in nucleocapsid assembly, albeit the underlying mechanism and the relevance of NP-NP interaction in nucleocapsid activity are still poorly understood. Here, we evaluate the contribution of the New World Tacaribe virus (TCRV) NP self-interaction to nucleocapsid functional activity. We show that alanine substitution of N-terminal residues predicted to be available for NP-NP interaction strongly affected NP self-association, as determined by coimmunoprecipitation assays, produced a drastic inhibition of transcription and replication of a TCRV minigenome RNA, and impaired NP binding to RNA. Mutagenesis and functional analysis also revealed that, while dispensable for NP self-interaction, key amino acids at the C-terminal domain were essential for RNA synthesis. Furthermore, mutations at these C-terminal residues rendered NP unable to bind RNA both *in vivo* and *in vitro* but had no effect on the interaction with the L polymerase. In addition, while all oligomerization-defective variants tested exhibited unaltered capacities to sustain NP-L interaction, NP deletion mutants were fully incompetent to bind L, suggesting that, whereas NP self-association is dispensable, the integrity of both the N-terminal and C-terminal domains is required for binding the L polymerase. Overall, our results suggest that NP self-interaction mediated by the N-terminal domain may play a critical role in TCRV nucleocapsid assembly and activity and that the C-terminal domain of NP is implicated in RNA binding.

IMPORTANCE

The mechanism of arenavirus functional nucleocapsid assembly is still poorly understood. No detailed information is available on the nucleocapsid structure, and the regions of full-length NP involved in binding to viral RNA remain to be determined. In this report, novel findings are provided on critical interactions between the viral ribonucleoprotein components. We identify several amino acid residues in both the N-terminal and C-terminal domains of TCRV NP that differentially contribute to NP-NP and NP-RNA interactions and analyze their relevance for binding of NP to the L polymerase and for nucleocapsid activity. Our results provide insight into the contribution of NP self-interaction to RNP assembly and activity and reveal the involvement of the NP C-terminal domain in RNA binding.

Viruses belonging to the *Arenaviridae* family are classified into two main groups, Old World (OW) and New World (NW), according to phylogeny, serological properties, and geographical distribution (1). Several members of this family, such as the NW Junin virus (JUNV) and the OW Lassa virus (LASV), produce serious hemorrhagic fever in humans. Tacaribe virus (TCRV), the prototype of NW arenaviruses, is nonpathogenic, closely related to JUNV, and has been used as a model in numerous studies (1–4). Arenaviruses are enveloped, and their genome is organized in two single-stranded negative-sense RNA segments, called S and L. Both genomic RNAs exhibit an ambisense strategy to encode two proteins: (i) the RNA-dependent RNA polymerase (L protein) and the matrix Z protein in the L RNA and (ii) the precursor of the envelope glycoproteins (GPC) and the nucleoprotein (NP) in the S RNA (2, 5).

NP is the most abundant viral protein in both infected cells and virions and exhibits multiple functions throughout the viral life cycle. Association of NP with the viral RNA segments not only confers protection to the genome but also is essential for synthesis of viral RNA. Indeed, multiple copies of NP associate with the viral genomic and antigenomic RNAs forming ribonucleoprotein (RNP) complexes called nucleocapsids, which along with the L polymerase are the biologically active units for transcription of nonencapsidated, subgenomic viral mRNAs and for viral genome replication (6–8). Besides, interaction between NP and the matrix Z protein has been shown to be an important element for packaging of RNPs into viral particles during virion morphogenesis (9–13). Arenavirus NP has also been linked to inhibition of type I interferon induction (14–19) and in the case of JUNV, NP has been proposed to act as a decoy substrate for apoptosis inhibition in infected cells (20).

Received 31 January 2014 **Accepted** 18 March 2014
Published ahead of print 2 April 2014
Editor: S. R. Ross
Address correspondence to Nora Lopez, nlopezcevan@centromilstein.org.ar.
* Present address: Maria Eugenia Loureiro, University of California, San Diego, Division of Biological Sciences, La Jolla, California, USA.

doi:10.1128/JVI.00321-14

The crystal structure of full-length NP, determined for a unique member of the *Arenaviridae* family, LASV, revealed that this protein is composed of two folding domains: N terminal (N-ter [residues 1 to 338]) and C terminal (C-ter [residues 364 to 569]) (21, 22). Furthermore, recombinant LASV NP purified from bacteria or insect cells was crystallized as an RNA-free trimer exhibiting two possible conformations (21, 22). One is a symmetric trimer displaying a head-to-tail (N-ter-to-C-ter) arrangement of monomers; the alternative configuration (asymmetric trimer) consists of two chains exhibiting a head-to-head (N-ter-to-N-ter) dimerization interface, which are loosely connected with the third NP monomer. In solution, the predominant conformation was identified as being similar to the symmetric trimer (21). Binding of RNA to the LASV NP monomer has been predicted in a positively charged groove between the N- and C-terminal domains (22). Also, crystal structures of the N-ter domain of LASV NP in complex with RNA have shown the RNA bound in a basic crevice between the head and body regions that comprise this domain (23). However, no structural information is available on full-length NP in complex with RNA, and the participation of the C-ter domain in binding to viral RNA remains to be determined.

By means of mutagenesis analysis, we previously defined two (N-ter and C-ter) independent functional domains within TCRV NP, which is consistent with the two-domain structure described simultaneously for the full-length LASV NP monomer. Our studies demonstrated that TCRV NP is able to self-oligomerize with a yet undefined molecularity and identified the N-ter domain (residues 1 to 332) as being essential for NP self-interaction (11). Biochemical evidence supporting the relevance of the N-ter domain in self-association has also been reported for the NP of the OW arenaviruses lymphocytic choriomeningitis virus (LCMV) and LASV (24, 25). Although NP homo-oligomerization is presumed to play a role in assembly of viral nucleocapsids, the underlying mechanism and the role of NP self-association in the multiple activities of the RNP remain poorly understood.

Here, we report evidence demonstrating a distinct critical role of specific TCRV NP N-terminal and C-terminal amino acid residues in self-interaction and viral nucleocapsid functional activity. By combining mutagenesis analysis and biochemical and functional assays, we identify several N-terminal residues that are essential for NP-NP interaction and for the participation of NP in sustaining RNA transcription and replication mediated by the L polymerase, as well as for RNA binding. Our results also reveal that key C-terminal residues that are not required for NP self-association are critically important for RNA binding. Additionally, our findings provide novel insight into the requirements of the interaction between NP and the L polymerase.

MATERIALS AND METHODS

Cells and virus. BSR (a clone of BHK-21) and CV1 cells were grown in a 5% CO_2 atmosphere at 37°C, using Glasgow minimum essential medium (GMEM; Invitrogen) and Dulbecco's modified Eagle's medium (DMEM; Invitrogen), respectively. Growth media were supplemented with glutamine (2 mM), 10% fetal calf serum (FCS) (Invitrogen), and penicillin (100 U/ml)-streptomycin (100 μg/ml) (Invitrogen). Recombinant vaccinia virus vTF7-3, which expresses the T7 RNA polymerase (26), was kindly provided by Bernard Moss (National Institutes of Health, Bethesda, MD).

Plasmids. Plasmids expressing the Flag- or c-Myc-tagged versions of TCRV NP (pTCRV N-Flag and pTCRV N-myc, respectively) and plasmids pNΔ1–359, pNΔ334–476, and pNΔ477–570, which express TCRV NP deletion mutants, were generated previously (9, 11). Amino acid substitutions were introduced in the TCRV NP full-length sequence using a QuikChange site-directed mutagenesis kit (Stratagene), with pTCRV N-Flag as the template and primers containing the mutated sequences. The pTM1 vector-based plasmid pTacV L (referred to as "pTCRV L" hereafter) encoding the TCRV L protein was constructed previously (9). Plasmid pS-CAT expresses a minigenome (MG) RNA, here designated "MG-CAT," which is an analogue to the TCRV S genomic segment. This MG comprises the complete S genome 5′ untranslated region (UTR) followed by a linker sequence, the S intergenic region, the chloramphenicol acetyltransferase (CAT) open reading frame (ORF) in an antisense orientation, and the complete S genome 3′ UTR (9). Plasmid pMG-FLUC expresses an MG (designated "MG-FLUC") that includes the firefly luciferase (FLUC) reporter gene in the negative sense. To generate plasmid pMG-FLUC, the CAT ORF was replaced by the FLUC coding sequence in plasmid pS-CAT by standard PCR and cloning methods. Plasmid pGenCAT, which expresses an MG (GenCAT) containing the negative-sense copy of the CAT reporter gene flanked by the TCRV S 5′ and 3′ UTRs (8), was modified as follows. A KpnI site was first introduced downstream of the 3′ end of the MG sequence by site-directed mutagenesis. Next, a 461-bp fragment of the CAT sequence was deleted from the mutated construction by cleavage with EcoRI, followed by treatment with Klenow to fill in the ends, digestion with SnaBI, and gel purification and religation of the largest fragment. The resulting plasmid, pGenCATΔ, encodes a truncated version of MG GenCAT (designated MG-CATΔ) that was employed as bait for *in vitro* RNA-binding assays (see below). All constructs were checked by dideoxynucleotide double-stranded DNA sequencing (Macrogen, Inc.). All primer sequences and vector maps are available upon request. Plasmid pCMV-T7pol expresses the bacteriophage T7 RNA polymerase under cytomegalovirus promoter control (27) and was kindly provided by Martin A. Billeter (University of Zurich, Irchel, Switzerland).

DNA transfections. Mammalian cell monolayers grown in 12-well plates were transfected with the indicated amounts and combinations of plasmids using Lipofectamine 2000 reagent (Invitrogen), according to the manufacturer's instructions. Expression of viral proteins from transfected plasmids was driven by the T7 RNA polymerase supplied in *trans*. To this, transfections of BSR cells always included 1 μg of pCMV-T7pol per well, and transfections of CV1 cells were preceded by infection with vTF7-3 (3 to 5 PFU per cell) for 1 h at 37°C, as described before (8). In all transfections, the total amount of transfected DNA was kept constant by the addition of empty pTM1 vector DNA.

Analysis of protein-protein interactions by coimmunoprecipitation. For NP-NP interaction analysis, vTF7-3-infected CV1 cell monolayers were transfected with 3 μg of pTCRV N-myc and 3 μg of pTCRV N-Flag or each of the indicated NP mutant-expressing plasmids. At 24 h posttransfection (hpt), cells were washed with 1× phosphate-buffered saline (PBS) and then lysed in buffer TNE-N (50 mM Tris [pH 7.4], 150 mM NaCl, 1 mM EDTA, 0.5 mM dithiothreitol, 0.2% Nonidet P-40) containing protease inhibitors (20 μg/ml phenylmethylsulfonyl fluoride, 50 μg/ml *N*-α-tosyl-L-lysine chloromethyl ketone [Sigma-Aldrich]). Cell lysates were clarified by centrifugation at 16,000 × *g* for 20 min at 4°C. Aliquots of cytoplasmic extracts (corresponding to about 2×10^5 cells) were immunoprecipitated with either rabbit anti-c-Myc polyclonal antibody (Santa Cruz Biotechnology) or mouse anti-Flag M2 monoclonal antibody (MAb) (Sigma-Aldrich), using protein A-Sepharose CL-4B Fast Flow (Sigma-Aldrich), as previously described (28).

For NP-L interaction analysis, vTF7-3-infected CV1 cells were transfected with 3 μg of pTCRV L or were cotransfected with 3 μg of pS-CAT and 3 μg of pTCRV N-Flag or each of the indicated NP mutant-expressing plasmids. Cells were lysed at 24 hpt as indicated above. Then lysates from pTCRV L-transfected cells were pooled, and an aliquot (corresponding to about 4×10^5 cells) was combined with an equivalent amount of lysate from cells expressing either wild-type (WT) or mutant NP or, as a control, from mock-transfected cells. Mixtures were incubated overnight at 4°C with constant rocking. Then protein complexes were immunoprecipi-

tated with a rabbit anti-L polyclonal antibody (29) and protein A-Sepharose beads, as indicated above. To control for unspecific binding of NP to protein A-beads, an aliquot of lysate containing WT NP was mixed with an equal volume of mock-transfected cell lysate and subjected to the same incubation procedure, in the absence of anti-L antibody.

All immunoprecipitation experiments were followed by analysis of the precipitated proteins by Western blotting.

Western blotting. Proteins were resolved by SDS-PAGE in gels containing 10% (for NP) or 8% (for L) polyacrylamide and then transferred to a nitrocellulose membrane (Hybond-ECL; GE Healthcare). Blots were stained with Ponceau-S (Sigma-Aldrich) to control for gel loading and correct transference (data not shown). Immunodetection was performed according to a protocol previously described (9), employing rabbit anti-c-Myc antibody, mouse anti-Flag M2 MAb, anti-TCRV L, or a rabbit anti-TCRV NP polyclonal serum (29) as the primary antibody. Horseradish peroxidase-conjugated anti-mouse or anti-rabbit secondary antibodies (Jackson ImmunoResearch) were used according to the supplier's specifications. Protein bands were visualized with SuperSignal West Pico chemiluminescent substrate (Thermo Scientific) and quantified by densitometry using ImageJ software (30).

MG assay. The experimental conditions set for intracellular MG transcription and replication were previously reported (9). Briefly, BSR cells were transfected in duplicates with (per well) 3 μg of plasmid pMG-FLUC and 1 μg of pTCRV L along with 3 μg of either pTCRV N-Flag or each of the NP mutant-expressing plasmids. To control for transfection efficiency, 80 ng per well of the *Renilla* luciferase (RLUC) reporter vector phRL-TK (Promega) was added to the transfection mixture. At 4 hpt, supernatants were removed and cells were washed twice with 1× PBS and further incubated with GMEM containing 2% FCS for 48 h at 37°C. Cell lysis and quantification of FLUC and RLUC activities on a Biotek FLx800 luminometer were performed using a Promega dual-luciferase reporter assay system according to the manufacturer's instructions. For each sample, FLUC activity was normalized against RLUC activity. The mean value determined for cells coexpressing MG-FLUC and L with wild-type NP was defined as 100%.

Northern blot Analysis. BSR cells were transfected to allow MG transcription and replication under the conditions described above, with the exception that plasmid pMG-FLUC was replaced by plasmid pS-CAT at the same amounts. Total cellular RNA was purified at 24 hpt using TRIzol reagent (Invitrogen), following the manufacturer's instructions. One microgram of purified RNA was resolved per lane on 1.5% agarose–MOPS (morpholinepropanesulfonic acid) gels containing 2.2 M formaldehyde. At the end of the run, ribosomal RNAs were UV visualized upon gel staining with ethidium bromide. RNA transference to a positively charged nylon Hybond-N membrane (Roche) and detection of either miniantigenome and CAT mRNA or minigenome with *in vitro*-synthesized ^{32}P-labeled CAT riboprobes was performed as described previously (8).

***In vivo* RNA encapsidation assay.** CV1 cells were transfected with (per well) 3 μg of plasmid pS-CAT and 3 μg of either pTCRV N-Flag or the indicated NP mutant-expressing plasmid. At 24 hpt, cells were lysed in buffer TNE-N containing protease inhibitors and clarified, as described above. Cell lysates were incubated with anti-NP antibody-coupled protein A-Sepharose 4B Fast Flow, and immunocomplexes were collected by centrifugation, as previously reported (8). Then immunocomplexes were treated with TRIzol (Invitrogen) to isolate both RNA and proteins, as indicated by the manufacturer. The RNA was ethanol precipitated from the aqueous phase after addition of 1 μg of total RNA from mock-infected CV1 cells as carrier, which also served as an internal control for the following step. Purified RNA was retrotranscribed with SuperScript reverse transcriptase (Invitrogen) using a CAT-specific primer and a primer specific for the glyceraldehyde-3-phosphate dehydrogenase (GAPDH) housekeeping gene. The resulting cDNA was employed as the template to amplify either a CAT- or a GAPDH-specific 110-bp DNA fragment by real-time PCR using Power SYBR green (Invitrogen). Amplification reactions were run in triplicate under the following conditions: 10 min at 95°C followed by 40 cycles of 94°C for 15 s and 60°C for 60 s. For each sample, average threshold cycle (C_T) values determined for CAT were normalized to the average C_T values for GAPDH. The level of MG-CAT RNA associated with mutant NP relative to the amount of MG-CAT RNA encapsidated by wild-type NP was estimated using the $2^{-\Delta\Delta CT}$ equation. Gene-specific primers were designed with the Primer Express software (Applied Biosystems); sequences are available upon request.

***In vitro* RNA-binding assay.** Plasmid pGenCATΔ was linearized with KpnI followed by Klenow fragment treatment to remove overhanging nucleotides and then purified by phenol-chloroform extraction and ethanol precipitation. Linearized pGenCATΔ DNA was used as the template for *in vitro* transcription employing a T7 RNA polymerase-based transcription kit (MegaScript-Ambion). The RNA transcript (MG-CATΔ), which contains the complete TCRV S 5′ and 3′ UTRs flanking a truncated version of the CAT gene, was purified by Illustra MicroSpin G-50 columns (GE Healthcare Life Sciences) and then immobilized onto agarose beads according to a well-established procedure (31, 32). Briefly, 10 μg of synthetic RNA was activated by incubation in 5 mM sodium *m*-periodate (Sigma-Aldrich)–100 mM sodium acetate (pH 5.0) for 1 h at room temperature in the dark. After ethanol precipitation, the RNA was resuspended in 500 μl of 100 mM sodium acetate (pH 5.0) and mixed with 300 μl of a 50% slurry of adipic acid dihydrazide-agarose beads (Sigma-Aldrich) previously equilibrated in 100 mM sodium acetate (pH 5.0). Following incubation for 18 h at 4°C with constant rotation, RNA-coupled beads were pelleted by centrifugation, extensively washed (three times with 1 ml of 2 M NaCl plus three times with 1 ml of TNE-N containing protease inhibitors), and resuspended in 300 μl of the final washing buffer. Fifty microliters of the RNA-bead slurry was mixed with aliquots (corresponding to about 4×10^5 cells) of lysates from CV1 cells expressing either wild-type or mutant NP as indicated and then incubated overnight at 4°C. Protein-RNA-bead complexes were collected after low-speed centrifugation for 2 min, washed four times with 1 ml of TNE-N, and pelleted by a final centrifugation step. Proteins bound to the immobilized RNA were eluted by addition of 25 μl of 3× SDS-PAGE loading buffer and analyzed by Western blotting to detect NP.

Sequence analysis and prediction of TCRV NP structure. All arenavirus sequences were retrieved by BLAST, using TCRV NP (Uniprot accession no. L7X3T1_TACV; www.uniprot.org/uniprot/L7X3T1) as the query in the NCBI nonredundant database. Multiple sequence alignments were done by t_coffee (33) on a set of 116 nonredundant NP sequences and on a subset of 23 representative NP sequences. Amino acid conservation scores were retrieved at the ConSurf server (http://consurf.tau.ac.il/index_proteins.php). Both alignments gave comparable conservation scores at the positions analyzed. Data are available upon request.

A three-dimensional (3D) model of TCRV NP (Uniprot accession no. L7X3T1_TACV), restricted to the region comprised between residues 7 and 563, was created with MODELLER (34, 35), based on the full-length LASV NP crystal structure (Protein Data Bank [PDB] code 3MWP) (22). Validation of the model was carried out by ProSA (36) and Verify3d (37). Also, the stereochemical quality of the model was assessed by Ramachandran plot using PROCHECK (38). Superimposition (39) with 3MWP gave a global root mean square deviation (RMSD) of 0.352 Å across 506 equivalent positions. The symmetric trimer of TCRV NP was modeled using PDB coordinates kindly provided by Markus Perbandt (University of Hamburg) as the template. Modeling of the TCRV NP asymmetric trimer was based on the X-ray structure 3MWP. The methodology described above was also employed to generate and validate the molecular model of the TCRV NP N-terminal domain based on the structure of the LASV NP N-ter domain bound to RNA (PDB code 3T5N) (23). The N-terminal structure gave a global RMSD of 0.36 Å across 281 equivalent positions. All of the evaluations supported the correctness of the models.

RESULTS

Effect of N-terminal and C-terminal mutations on TCRV NP self-interaction. Previous studies on TCRV and LCMV demon-

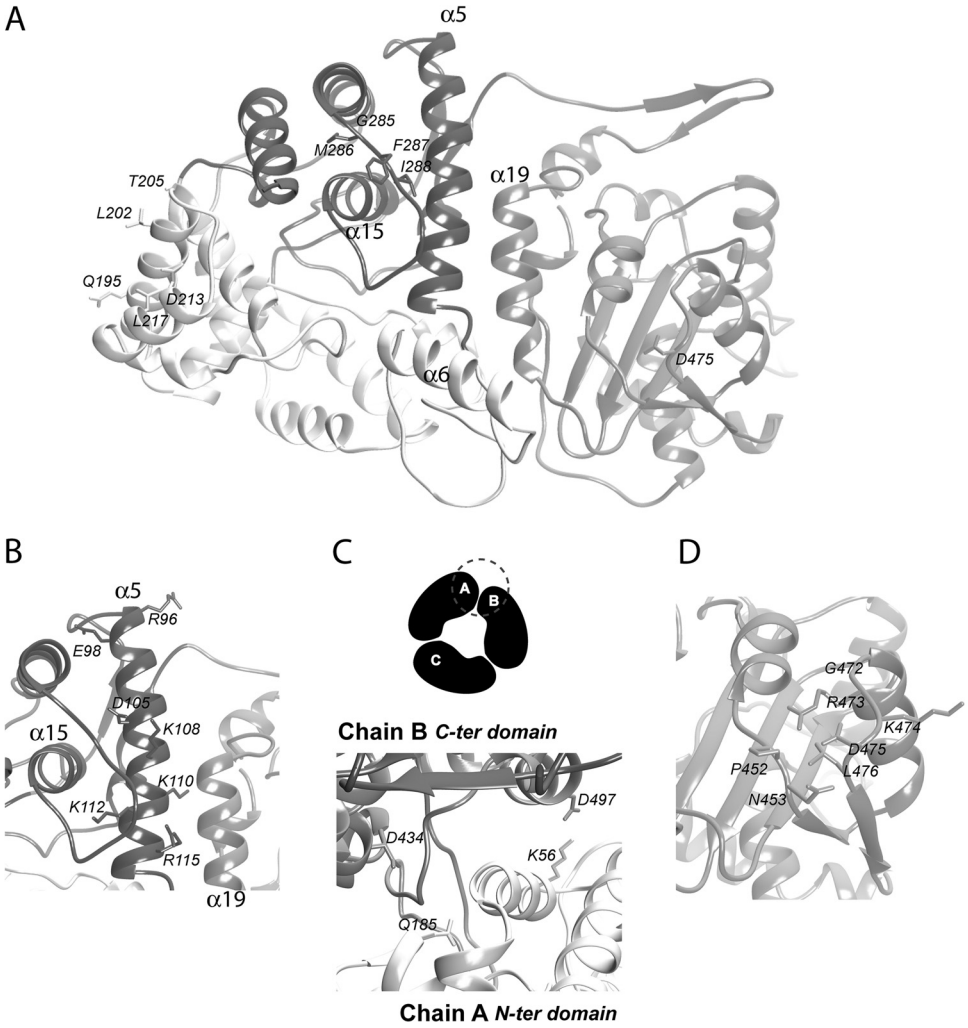

FIG 1 Location of amino acid residues selected as targets for mutagenesis in the TCRV NP model. (A) The modeled NP monomer is shown as a ribbon diagram; relevant residues at the protein surface are indicated. (B) Ribbon representation centered at α-helix 5. (C) (Top) Schematic representation of the NP symmetric trimer; the head-to-tail intermonomeric interface is indicated with a dashed circle. (Bottom) Predicted interface between monomers A and B, rendered as ribbons. (D) Ribbon representation centered at the NP C-ter domain. The mutated residues are located outside the head-to-tail interface. (A to D) The head and body regions of the N-ter domain and the C-ter domain are shown in dark gray, white, and light gray, respectively. Mutated amino acid residues are shown as sticks. In panels A and B, N-terminal α-helices 5 (α5), 6, and 15 and C-terminal α-helix 19 are indicated.

strated that NP self-associates in mammalian cells into oligomers and that the NP N-ter domain plays a relevant role in homo-oligomerization (11, 24). Furthermore, a 28-residue region predicted to fold into an α-helix (helix 5) within the N-ter domain was identified as being essential to sustain TCRV NP self-association (11). However, the mechanism by which NP homo-oligomerization contributes to RNP assembly as well as to viral transcription and replication remains unclear. In order to investigate the impact of TCRV NP self-interaction in active nucleocapsid assembly, and based on these precedents, we first aimed at further defining N-terminal residues engaged in NP-NP contacts and evaluating their participation in RNA synthesis. Considering that no full-length structure of any NW arenavirus NP is already available, we generated molecular models of both the monomer and the symmetric trimer of TCRV NP employing the 3D structure of LASV NP (50% sequence identity) as the template. On the basis of the location in these models as well as on the conservation score of individual positions across the *Arenaviridae* in multiple sequence alignments (data not shown), amino acid residues that were candidates for mutagenesis were identified at both the head and body regions of the N-ter domain (Fig. 1A and 2A). Specifically, three sets of targets were selected. One of them comprises residues located at the protein surface outside any interface found in the trimer. Within this group, the strictly conserved amino acids M286 and F287 and nearby positions were mutated to obtain the NP G285A/M286A, F287A/I288A, and D290A/R291A variants. Likewise, a set of highly conserved amino acid residues, Q195, L202, T205, D213, and L217, also potentially accessible for NP-NP interactions, were individually replaced by alanine (Fig. 1A). A second set of single- or double-point alanine substitutions were introduced at conserved charged residues within α-helix 5 to generate the R96A/E98A, D105A/K108A, K110A, K110A/K112A and R115A mutants (Fig. 1B). Finally, a third group of selected targets included residues K56 and Q185, which lie at the presumed

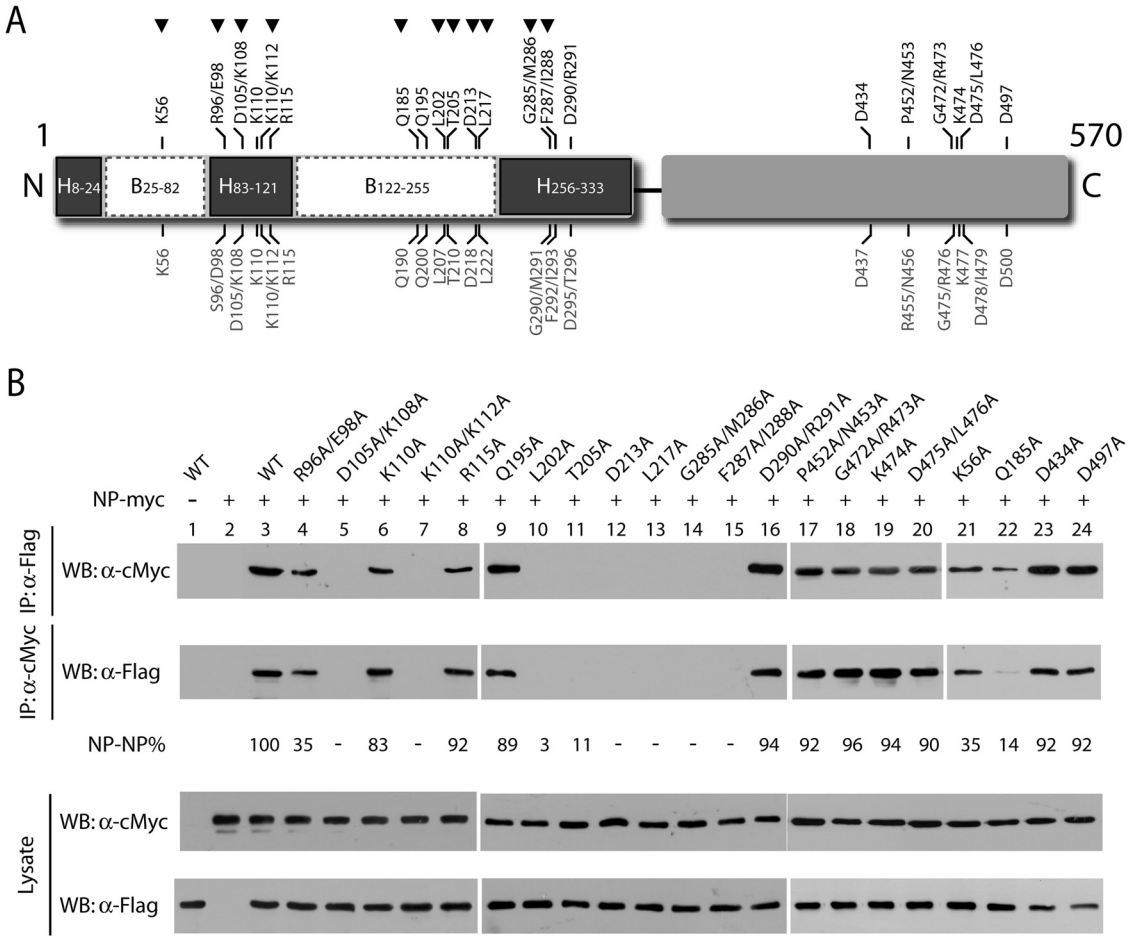

FIG 2 Identification of amino acids critical for TCRV NP self-interaction. (A) Schematic representation of wild-type TCRV NP. Numbers on top indicate positions on the TCRV NP amino acid sequence that were replaced by alanine. The numbering of the corresponding residues on LASV NP sequence is indicated below the scheme. Boxes represent regions comprised in the head (H, dark gray) or the body (B, white) of the N-ter domain; numbers indicate their boundaries. The C-ter domain is represented with a light gray box. (B) CV1 cells were transfected to express a c-Myc-tagged version of wild-type TCRV NP (NP-myc) and either NP-Flag (WT) or each of the indicated Flag-tagged NP mutants. As a control, NP-Flag and NP-myc were expressed alone (lanes 1 and 2). Cell extracts obtained at 24 hpt were immunoprecipitated using either anti-Flag (IP: α-Flag) or anti-c-Myc (IP: α-cMyc) antibody. Precipitated proteins (IP panels) and aliquots of input cell lysates were examined by Western blotting, using anti-Flag (WB: α-Flag) or anti-c-Myc (WB: α-cMyc) antibody, as indicated. To estimate NP self-interaction (NP-NP%), the amount of NP-Flag (WT or mutant) coimmunoprecipitated with NP-myc using anti-c-Myc antibody was normalized for NP-Flag (WT or mutant) expression. Conversely, the amount of NP-myc coimmunoprecipitated with NP-Flag (WT or mutant) using anti-Flag antibody was normalized for NP-myc expression. For each set of data (IP: α-cMyc and IP: α-Flag), the ratio calculated for each mutant was expressed as a percentage of that calculated for the WT, taken as 100%. Mean values from at least two independent experiments are presented; standard deviations ranged from 0 to 12%, except for the R96A/E98A, Q185A, L202A, and T205A mutants, which displayed self-interaction values of 35% ± 11%, 14% ± 8%, 3% ± 1%, and 11% ± 3%, respectively. (−), undetectable; α, anti. Arrowheads on top in panel A show the mutations associated with the self-association-defective phenotype.

head-to-tail interface within the trimeric model (Fig. 1C). Wild-type and mutant NPs were expressed fused to the Flag epitope at the N terminus, as we have previously shown that Flag-tagged TCRV NP (NP-Flag) is fully functional in a minireplicon system (9). Subsequently, the ability of mutant proteins to self-interact was evaluated by coimmunoprecipitation assays, as previously described (11). Briefly, a c-Myc-tagged version of TCRV NP was coexpressed with either wild-type NP-Flag or each of the NP variants in mammalian cells. Aliquots of the cell lysates were incubated with either anti-Flag or anti-c-Myc antibody, and the precipitated proteins were analyzed by Western blotting (Fig. 2B). Controls indicated that the antisera did not cross-react and that NP-myc coimmunoprecipitated with wild-type NP-Flag specifically (see lanes 1 to 3 in the immunoprecipitation [IP] and lysate panels). The results also showed that mutant proteins, which were expressed at levels similar to WT NP (lysate panels, lanes 4 to 24), displayed two distinct phenotypes. While a few NP mutants exhibited almost unmodified capacities to self-associate, ranging around 80 to 90% of that of the NP WT (the K110A, R115A, Q195A, and D290A/R291A mutants in lanes 6, 8, 9, and 16 in the IP panels), most mutations clearly reduced or abrogated NP-self-interaction (IP panels, lanes 4, 5, 7, 10 to 15, 21, and 22). Overall, these results confirmed the participation of the TCRV NP N-ter domain in self-association, suggesting that several residues located at the NP surface, being engaged or not in head-to-tail interactions in a putative trimer, as well as a subset of the examined residues placed at α-helix 5, are involved in NP-NP contacts.

Because the C-terminal residue D471, which is strictly conserved across the *Arenaviridae*, has been recently reported to be essential for homo-oligomerization of LCMV NP (40), we next

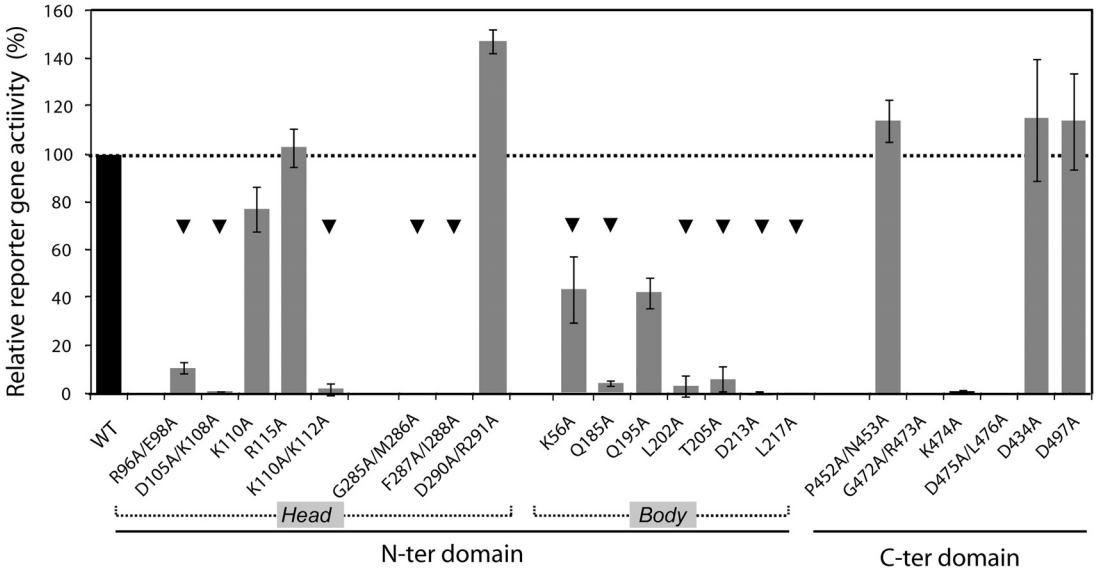

FIG 3 Effect of NP mutations on TCRV minigenome expression. Duplicate monolayers of BSR cells were transfected with the MG-FLUC-expressing plasmid and pTCRV L, along with pTCRV N-Flag or each of the indicated NP mutant-expressing plasmids. All transfection mixtures included a plasmid expressing *Renilla* luciferase (RLUC) to control for transfection efficiency. In control cell monolayers, plasmid pTCRV L was omitted. Cytoplasmic extracts obtained at 48 hpt were used to measure FLUC and RLUC activities; FLUC activity data were normalized against the corresponding RLUC levels, as indicated in Materials and Methods. Normalized FLUC background levels, determined in extracts from control cells expressing MG-FLUC and NP WT in the absence of L (data not shown), were subtracted from all normalized data. Mean values (±standard deviations) from three independent experiments are shown as a percentage of those corresponding to wild-type NP, taken as 100%. Arrowheads indicate values corresponding to the self-association-defective mutants characterized in Fig. 2.

sought to analyze the involvement of the corresponding position (D475) and its local environment in TCRV NP-NP contacts. To this end, a double-alanine substitution was engineered to obtain the TCRV NP D475A/L476A mutant. Residues G472, R473, and K474, placed at the loop harboring amino acid D475, as well as nearby residues P452 and N453, located in the neighboring loop (Fig. 1D), were mutated to generate NP G472A/R473A, K474A, and P452A/N453A variants. Likewise, alanine substitutions were introduced within the C-ter domain at conserved residues D434 and D497, which are located far apart from D475 and predicted to be placed at the head-to-tail interface in the TCRV NP trimeric model (Fig. 1C). When analyzed by coimmunoprecipitation, all C-terminal mutants displayed unaltered self-binding capacities compared to the NP WT (Fig. 2B, IP panels, lanes 17 to 20, 23, and 24). Thus, the C-terminal residue D475, corresponding to LCMV NP D471, and those in its vicinity (G472, R473, K474, L476, P452, and N453), as well as distant, conserved residues D434 and D497, appear to be unnecessary for TCRV NP-NP interactions.

Effect of NP mutations on RNA synthesis, interaction of NP with the L polymerase, and NP binding to RNA. Based on the hypothesis that NP oligomerization must be essential for viral RNA encapsidation, disruption of NP-NP contacts is expected to cause impairment in the synthesis of viral RNA. However, there is still little evidence on how NP self-association impacts viral replication and transcription. To shed light on this, we examined the ability of NP mutants to support viral RNA synthesis (Fig. 3). To this end, we used a TCRV minigenome system, in which NP and L proteins are sufficient to promote full-cycle replication of S RNA genome analogs (8, 9, 41). Plasmid pMG-FLUC was designed to encode a minigenome (MG-FLUC) containing the firefly luciferase reporter gene and the complete TCRV S RNA noncoding sequences (Materials and Methods). As expected, coexpression of MG-FLUC along with TCRV L and NP WT resulted in high levels of luciferase activity, while omission of the L protein caused reporter gene expression to drop to levels less than 1% of those in the presence of L (see the legend to Fig. 3). N-terminal mutants that exhibited impaired or markedly reduced capacities to self-associate (K56A, R96A/E98A, D105A/K108A, K110A/K112A, Q185A, G202A, T205A, D213A, L217A, G285A/M286A, and F287A/I288A variants) mediated reduced or background levels of reporter gene activity (marked with arrowheads in Fig. 3). In contrast, with the exception of the Q195A mutant, which had a limited capacity to promote minigenome expression, NP mutants with changes at the N-ter domain that did not affect protein self-interaction, supported luciferase activity at levels similar to (K110A and R115A variants) or even higher than (D290A/R291A variant) those of wild-type NP. Overall, these results demonstrated that key residues pertaining to both the head and body regions of the N-ter domain and which are critically involved in NP self-association are also required for viral RNA synthesis, suggesting that they might therefore participate in protein-protein contacts relevant for active nucleocapsid assembly. Remarkably, mutations G472A/R473A, K474A, and D475A/L476A at the C-ter domain, which did not impact NP self-interaction, caused a severe inhibition in FLUC activity, while substitution at other C-terminal positions (P452, N453, D434, and D497) had no effect (Fig. 3). These results indicated that the C-terminal residues G472, R473, K474, D475, and L476 are critically involved in viral RNA synthesis.

Levels of reporter gene expression measured in the context of the TCRV minireplicon system reflect multiple rounds of transcription and replication of the virus RNA analog. Since mutations abrogating FLUC activity could be only preventing RNA transcription (and reporter gene expression) without altering

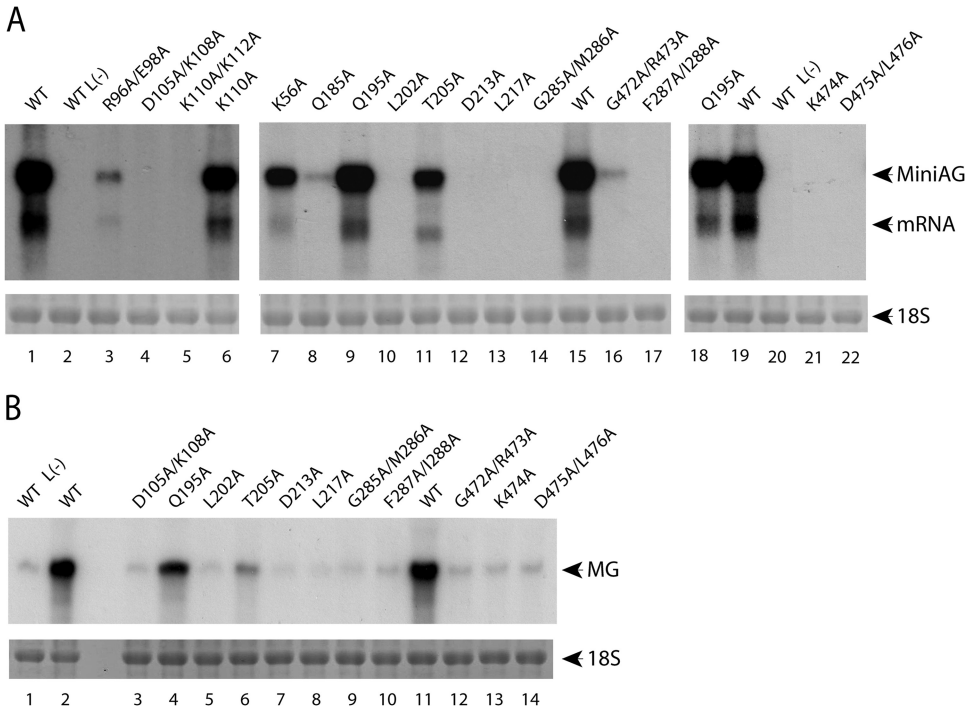

FIG 4 Analysis of the ability of NP mutants to support viral RNA transcription and replication. Subconfluent cultures of BSR cells were transfected with the MG-CAT-expressing vector (pS-CAT [Materials and Methods]), and pTCRV L along with either pTCRV N-Flag or each of the indicated NP mutant-expressing plasmids. In control cell monolayers, plasmid pTCRV L was omitted from the transfection mixture [L(−)]. Total intracellular RNA was purified and analyzed by Northern blotting using a negative-sense (A) or positive-sense (B) ^{32}P-labeled CAT riboprobe. In panels A and B, the lower panels show the ethidium bromide-stained 18S rRNA as a control for gel loading. The positions of mRNA, miniantigenome (MiniAG), or minigenome (MG) bands are indicated on the right. Blots in panel A were exposed longer than those in panel B to visualize the mRNA band.

RNA replication, we wanted to address the capacity of FLUC-negative NP mutants to promote transcription, replication, or both. To this end, mammalian cells were transfected to express MG-CAT (Materials and Methods) and L protein along with either NP WT or each of the NP mutants. Total cellular RNA was purified 24 h later, and accumulation of mRNA and miniantigenome was analyzed by Northern blotting using a strand-specific radiolabeled riboprobe that hybridizes to the CAT$^+$ sequence (Fig. 4A). RNA species corresponding to CAT mRNA and miniantigenome were clearly detected in cells expressing wild-type NP and L (lanes 1, 15, and 19) and were undetectable in the absence of L protein ["L(−)" in lanes 2 and 20], as expected. N-terminal NP variants that were defective for reporter gene expression mediated either reduced levels (K56A and T205A, lanes 7 and 11) or virtually no CAT mRNA and miniantigenome accumulation (R96A/E98A, D105A/K108A, K110A/K112A, Q185A, L202A, D213A, L217A, G285A/M286A, and F287A/I288A variants, lanes 3 to 5, 8, 10, 12 to 14, and 17). Similar results were obtained for C-terminal NP mutants unable to sustain FLUC expression, having the mutations G472A/R473A, K474A, and D475A/L476A (lanes 16, 21, and 22). The diminished replicative ability of most of these NP variants was confirmed upon analysis with a riboprobe complementary to the CAT$^-$ sequence. As depicted in Fig. 4B, nearly background levels of minigenome accumulation were mediated by the D105A/K108A, L202A, T205A, D213A, L217A, G285A/M286A, F287A/I288A, G472A/R473A, K474A, and D475A/L476A mutants (compare lanes 3, 5 to 10, and 12 to 14 to lane 1). Altogether, these results showed that mutations blocking the ability of NP to support reporter gene expression had an overall effect on RNA synthesis, impairing the capacity of NP to mediate both RNA transcription and replication.

Experimental data on TCRV and several Old World arenaviruses have demonstrated that L and NP proteins interact with each other (28, 42). Based on the assumption that NP-L interaction is essential for the activity of the RNP, the inability of NP mutants to support RNA synthesis may be caused by a disruption of the interaction with the L polymerase. To evaluate this possibility, representative NP mutants were examined for their capacities to interact with the L protein *in vitro*, in the presence of a TCRV RNA minigenome. NP variants defective for RNA synthesis and displaying either impaired or unaffected self-interaction capacities were selected for these experiments. In addition, the D497A mutant, exhibiting a wild-type phenotype for both functions, was included as control. Aliquots of a cytoplasmic extract pool from L-expressing cells were pairwise combined with lysates from cells coexpressing the MG-CAT minigenome and either wild-type or mutant NP. The mixtures were incubated with anti-L antibody; immunocomplexes were precipitated with agarose-coupled protein A and analyzed by Western blotting to detect NP (Fig. 5A). Analysis of input lysates by immunoblotting indicated that L protein and both the NP WT and NP mutants were expressed at readily detectable levels (lysate panel). These experimental conditions allowed us to confirm the specific interaction between NP and L, as the NP WT coprecipitated with anti-L antibody only when L protein was present in the lysate mixture, and no NP was detected when the anti-L antibody was omitted (IP panel, lanes 1

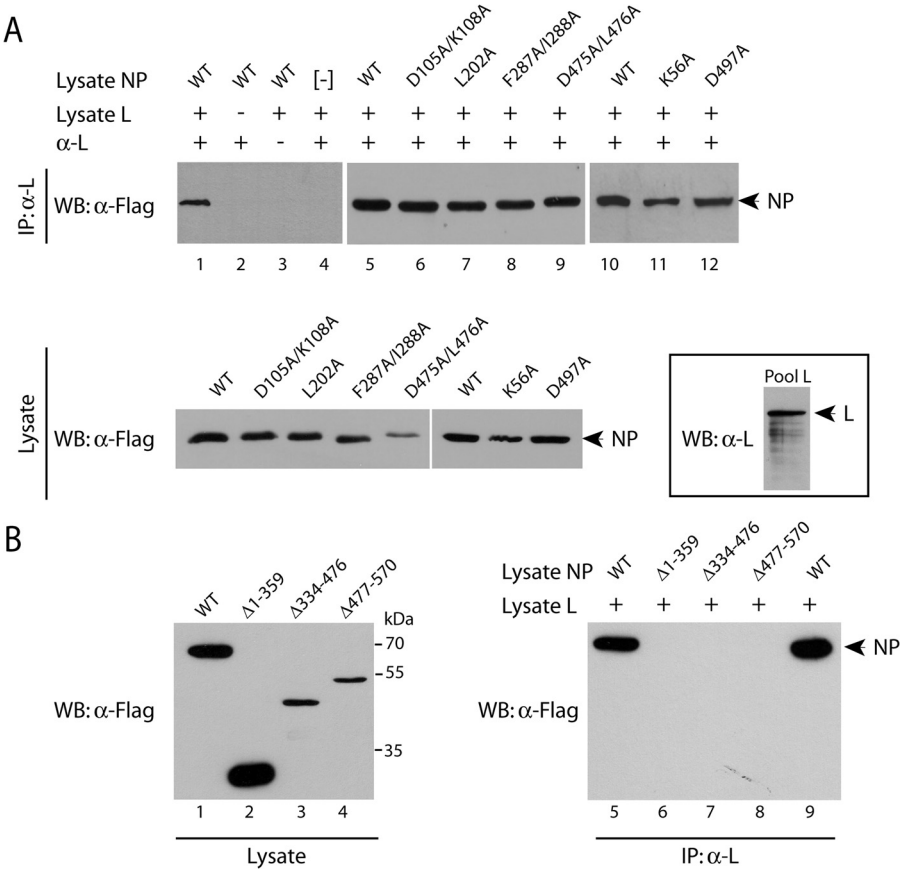

FIG 5 (A) NP point mutants are able to interact with the L polymerase. CV1 cells were transfected to express L or to coexpress the TCRV MG-CAT minigenome along with either NP WT or each of the indicated NP mutants. Control monolayers were mock transfected. In the IP panel, an aliquot of the L-expressing cell extract (pool L) was mixed with an equivalent amount of lysate from mock-transfected cells (lane 4) or from either wild-type- or mutant NP-expressing cells, as indicated on top. As a control, an aliquot of lysate containing NP WT was combined with an equivalent aliquot of mock-transfected cell extract (lane 2). Upon incubation for 16 h at 4°C, polyclonal anti-L serum (α-L) was added (+) or not (−) to each mixture, followed by immunoprecipitation with protein A-agarose. Precipitated proteins were analyzed by Western blotting using anti-Flag (WB: α-Flag) antibody. In the lysate panel, NP and L protein levels in transfected-cell lysates were analyzed by immunoblotting, using anti-Flag (WB: α-Flag) or anti-L (WB: α-L [inset]) antibody, respectively. (B) NP deletion variants fail to interact with L protein. CV1 cells were transfected to express L alone or to coexpress MG-CAT and either the NP WT or each of the indicated NP mutants. Immunoprecipitation of lysate mixtures containing L and NP (WT or mutant) with anti-L antibody and Western blotting of precipitated proteins and input lysates were carried out as in panel A. (The control for L protein expression is not shown.) The molecular masses of protein markers (in kDa) are indicated to the right of the lysate panel.

to 3). All of the NP mutants examined could precipitate with L protein at levels comparable to those of the NP WT (IP panel, compare lanes 6 to 9 with lane 5 and lanes 11 to 12 with lane 10). These results indicated that none of the substitutions affected NP-L interaction irrespective of whether they dampened RNA synthesis (D105A/K108A, L202A, F287A/I288A, D475A/L476A, and K56A) or not (D497A, lane 12). Additionally, the observation that probed NP variants deficient for self-interaction (D105A/K108A, L202A, F287A/I288A, and K56A) showed wild-type abilities to bind L suggested that these NP mutants are likely to preserve correct overall folding and that NP self-association is not strictly necessary for the interaction with the L polymerase.

To further characterize the NP-L interaction, previously generated Flag-tagged NP deletion mutants (11) were evaluated for their capacity to bind L. The Δ1–359 mutant, which lacks the entire N-ter domain, and mutants carrying deletions that span the complete C-terminal domain (Δ334–476 and Δ477–570) were tested in similar coimmunoprecipitation experiments (Fig. 5B). Expression of the NP WT and NP variants was confirmed by Western blotting of input lysates (lysate panel). Analysis of proteins immunoprecipitated with anti-L antibody revealed that the three NP variants failed to associate with L (IP panel, lanes 6 to 8), whereas the interaction between L and NP WT could be evidenced as expected (IP panel, lanes 5 and 9). These results indicated that deletion of the entire N-terminal domain or truncation of large regions in the C-terminal domain abrogates the interaction between NP and L, suggesting that both protein domains (N-ter and C-ter) are required for the interaction with the L polymerase.

We next asked whether failure of NP mutants to support RNA synthesis may be related to defective binding to RNA. To address this question, two RNA synthesis-defective NP variants that show distinct self-association phenotypes (L202A and D475A/L476A) were first evaluated for their RNA binding capacities in a cellular context. BSR cells were transfected to express MG-CAT along with either wild-type or mutant NP. As a control, cell monolayers were transfected to express MG-CAT and L protein in the absence of NP. Transfected-cell lysates were immunoprecipitated with an excess of anti-NP antibody coupled to protein A-agarose for recov-

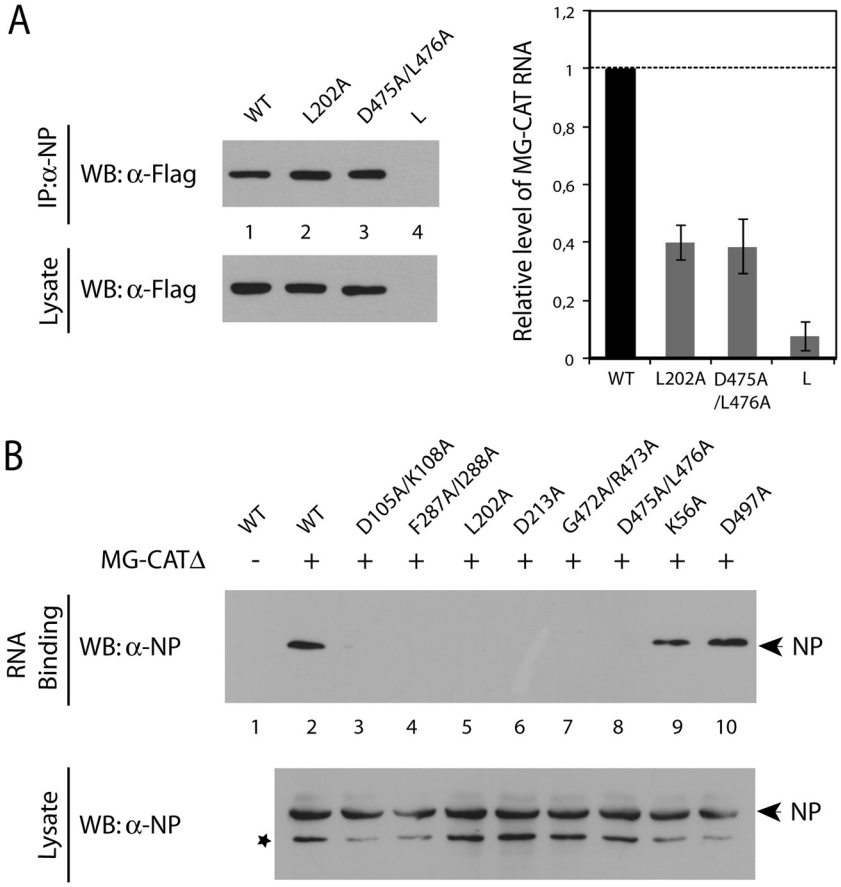

FIG 6 RNA binding assays. (A) CV1 cells were transfected with the MG-CAT-expressing plasmid, along with pTCRV N-Flag or the indicated NP mutant-expressing plasmids. Control monolayers were transfected to express MG-CAT and L protein in the absence of NP. An aliquot of the cell lysates, obtained at 24 hpt, was analyzed by Western blotting with anti-Flag antibody (WB: α-Flag [lysate panel]). Another aliquot was immunoprecipitated with anti-NP antibody-coupled protein A-agarose, and the precipitated complexes were subjected to RNA and protein extraction. In the IP panel, the protein fraction was analyzed by immunoblotting with anti-Flag antibody. For the bar graph, precipitated MG-CAT RNA was quantified by real-time RT-PCR. Mean values and standard deviations from 3 independent experiments are shown, presented as the level of MG-CAT RNA associated with mutant NP relative to that encapsidated by WT NP, defined as 1. (B) Monolayers of CV1 cells were transfected with 3 μg of the appropriate plasmid to express the NP WT or each of the indicated NP mutants and then lysed at 24 hpt. In the RNA binding panel, aliquots of the cell lysates were incubated with agarose beads previously coupled (+) or not (−) with *in vitro*-synthesized MG-CATΔ RNA (Materials and Methods), as indicated on top. Proteins bound to RNA-agarose complexes were analyzed by Western blotting using anti-NP serum (WB: α-NP). In the lysate panel, expression levels of wild-type and mutant NPs were examined by Western blotting using the anti-NP antibody. The asterisk denotes a degradation product of NP. Images in panel B are representative of at least two independent experiments.

ery of both free NP and NP-RNA complexes. Analysis by real-time RT-PCR of the RNA fraction isolated from immunocomplexes (Fig. 6A, bar graph) revealed levels of precipitated minigenome RNA from cells expressing either the L202A or D475A/L476A NP that were around 40% of those precipitated from wild-type NP-expressing cells. The specificity of the immunoprecipitation was demonstrated by the fact that only low levels of minigenome were precipitated from cells expressing L in the absence of NP (Fig. 6A, bar graph). Immunoblotting evaluation of input cell lysates confirmed that the NP WT and NP mutants were expressed at comparable levels (Fig. 6A, lysate panel), and analysis of the precipitated protein fraction demonstrated that NP was immunoprecipitated with similar efficiency from all samples (Fig. 6A, IP panel). Taken together, these results indicated that the L202A mutant, which is incompetent to self-associate, as well as the D475A/L476A mutant, displaying self-interaction ability comparable to that of the NP WT, similarly exhibited reduced capacities to bind RNA.

To further validate and extend our results, an *in vitro* RNA-binding assay was developed to assess the ability of NP mutants to interact with a single-stranded virus-like RNA. As described above, mutants inactive for RNA synthesis and either capable or unable to self-associate were evaluated in these experiments, and the D497A mutant was included as a control. Since we have previously demonstrated that the 5′ and 3′ UTRs of the S RNA contain all signals required in *cis* for minigenome encapsidation (8), we employed a synthetic RNA (MG-CATΔ), consisting of a truncated version of the CAT gene flanked by the complete TCRV S 5′ and 3′ UTRs, to be immobilized on agarose beads (Materials and Methods). RNA-agarose complexes were incubated with cytoplasmic extracts from cells expressing either WT or mutant NP. To control for non-RNA binding, bare agarose beads were incubated with an aliquot of the lysate containing the NP WT. Following extensive washing, beads were collected by centrifugation, and the associated NP was detected by Western blotting. As shown in Fig. 6B, the NP WT was readily precipitated with RNA-agarose

complexes through binding to the immobilized RNA, as no NP was captured upon incubation with agarose beads in the absence of RNA (RNA binding panel, lanes 1 and 2). Likewise, the D497A control mutant exhibited RNA binding capacities, determined as the ratio of precipitated NP to NP in the corresponding lysate, ranging around 130% that of the NP WT (lane 10). The K56A NP variant, having reduced replication and self-association activities, could bind RNA at nearly wild-type levels (lane 9). In contrast, the D105A/K108A, F287A/I288A, L202A, and D213A N-terminal mutants, which were fully defective for both RNA synthesis and self-interaction, failed to precipitate with the immobilized RNA (lanes 3 to 6). Notably, the results also showed that the G472A/R473A and D475A/L476A mutants, defective for replication and displaying wild-type abilities to self-associate, were unable to interact with MG-CATΔ RNA as well (RNA binding panel, lanes 7 and 8). Input levels of NP variants did not substantially differ from that of the NP WT (lysate panel). Taken together, these results indicated that while K56 would not be crucial, regions harboring residues D105, K108, L202, D213, F287, and I288 could contribute to RNA binding. Interestingly, the finding that mutations G472A/R473A and D475A/L476A disrupted the RNA binding ability of NP suggested that the C-ter domain of NP may be involved in the interaction with the viral RNA.

DISCUSSION

For several negative-strand RNA viruses, assembly of the RNP has been shown to involve nucleocapsid protein polymerization to enwrap the entire viral RNA genome (43–47). Arenavirus nucleoprotein homo-oligomerization, which has been documented for members of both the Old World (LASV and LCMV) and New World (TCRV) groups, has been proposed to be an essential element for arenavirus RNP assembly (11, 23–25). However, the mechanism involved and the role of NP self-interaction in RNP functionality remain poorly understood. To gain insight into the process of active nucleocapsid assembly, here we provide novel information on the interplay between NP-NP, NP-L, and NP-RNA interactions.

Importance of TCRV NP N-terminal residues for active RNP assembly. Because the N-terminal domain of NP from both TCRV and LCMV has been implicated in NP homo-oligomerization (11, 24), we started by characterizing the role of individual residues within the N-terminal domain, required for NP self-association, in competent nucleocapsid assembly. Due to the lack of the atomic structure of full-length NP from TCRV or any other NW arenavirus, we used a molecular model of TCRV NP based on the reported crystal structure of full-length LASV NP, to presume the location of individual residues both in the monomer and within a putative TCRV NP trimer. Also, we generated a molecular model of the TCRV NP N-terminal domain based on the structure of the LASV NP N-ter domain bound to RNA (23) as an approach to whether any of the mutated amino acids might be important for RNA binding.

For LASV NP, the C-terminal and N-terminal domains within each monomer have been reported to interact with each other. This interaction, involving α-helices 5 and 6 in the N-ter domain, has been suggested to contribute to the stability of NP trimer, which might represent a close arrangement keeping NP in an RNA-free form (23). Notably, we found that double-alanine substitution at positions within α-helix 5, R96/E98 and D105/K108, altered NP self-association and also impaired the capacity of NP to promote RNA transcription and replication (Fig. 2 to 4). The phenotype exhibited by these NP variants confirmed previous results indicating that a 28-residue region spanning α-helix 5 is required for TCRV NP self-interaction (11). Furthermore, these studies showed that hydrophobic residues (mostly leucine) arranged in a putative coiled-coil motif within this region, are important for NP-NP interaction (11). As in the TCRV NP model, these hydrophobic residues appear to be buried and are likely committed to local intradomain interactions (Fig. 7A); our previous observations may reflect the involvement of such residues in maintaining α-helix 5 stability and, probably, the overall N-ter domain folding. In contrast, amino acids R96, D105, and K108 are potentially available for interaction between the N-ter and C-ter domains in the modeled TCRV NP monomer (Fig. 7A). Hence, the phenotype of the R96A/E98A and D105A/K108A mutants would be consistent with observations on LASV NP supporting an important role of N-ter-to-C-ter intramonomeric interactions in RNA synthesis (23). Our finding that residues K110 and R115, also located at the predicted interface (Fig. 7A), are dispensable for TCRV NP self-association and RNA synthesis may imply that a distinct subset of amino acid residues are engaged in such intramonomeric contacts in phylogenetically distant arenavirus species.

In contrast to the wild-type phenotype exhibited by the K110A mutant, a double substitution of residues K110 and K112 abrogated NP self-association and RNA synthesis (Fig. 2 to 4), suggesting a critical role of amino acid K112. This residue, which is placed at α-helix 5 and strictly conserved across the *Arenaviridae*, appears to be in contact with the RNA in the LASV NP structure (PDB code 3T5N) and is also predicted to be in close proximity to the RNA in the modeled TCRV NP N-ter domain structure (Fig. 7B). Similarly, the strictly conserved amino acids M286 and F287 are comprised in a mobile loop close to α-helix 15 (Fig. 7B), the latter structure being part of the RNA-binding crevice in the N-ter domain (23). It seems likely that residues K112, M286, and F287 (and possibly G285 and I288) may be directly or indirectly involved in binding of TCRV NP to the RNA, a notion that appears to be supported by the RNA-binding-defective phenotype exhibited by the F287A/I288A mutant (Fig. 6). Considering this, the fact that mutations K110A/K112A, G285A/M286A, and F287A/I288A abolished NP self-association might suggest that RNA binding facilitates NP self-interaction.

In the case of LASV NP, a model has been proposed in which, in the context of the symmetric trimer, structural changes of NP, triggered by yet unknown factors, lead to RNA binding and nucleocapsid assembly. An implication of this model is that a protein-protein interaction or interactions other than the head-to-tail contacts observed in the LASV NP symmetric trimer structure may be relevant for RNA encapsidation. We found that the N-terminal residues L202, T205, D213, and L217 (Fig. 1A), which are highly conserved among the members of the *Arenaviridae*, are critically engaged in NP-NP interactions. Strikingly, examination of the TCRV NP molecular models showed that these amino acid residues do not participate in any intra- or intermonomeric interface in the putative symmetric trimer and that they do not contact RNA, but they lie at the head-to-head interface predicted in a hypothetical TCRV NP asymmetric trimer (Fig. 7C). Whether contacts involving these amino acids correspond to interactions in the RNP or arrangements of the RNA-free form of TCRV NP other than the symmetric trimer remains to be elucidated. In any case, the L202A, T205A, D213A, and L217A mutants displayed an

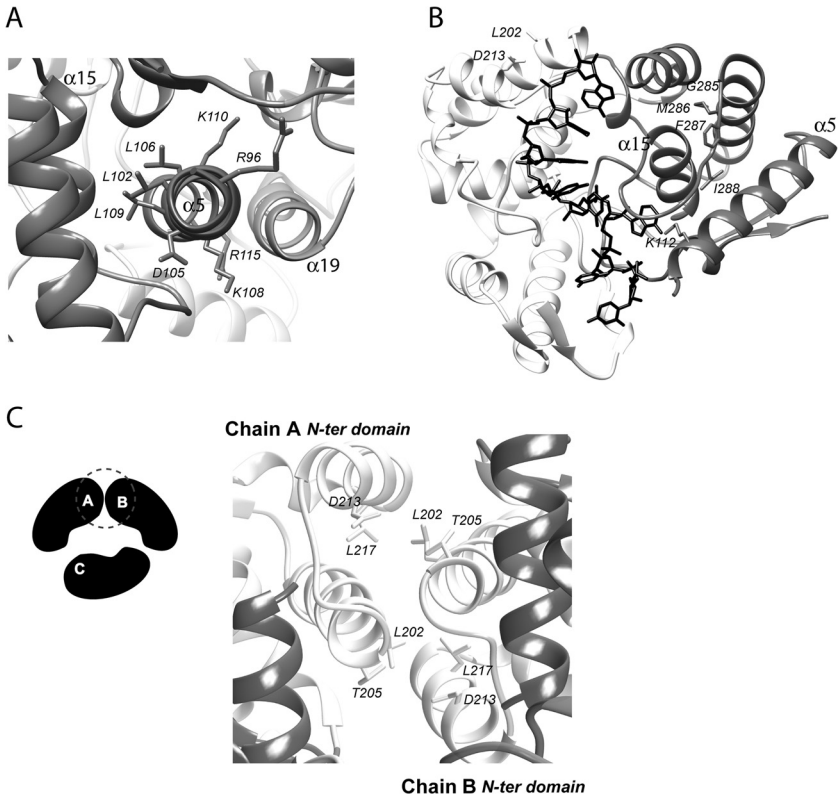

FIG 7 Predicted participation of TCRV NP N-terminal residues in inter- and intradomain contacts and RNA binding. (A) Zoomed-in view of the interface between the N-ter and C-ter domains within one NP monomer, rendered in ribbon form. The positions of hydrophobic (L) and charged (R, D, and K) residues within α-helix 5 are shown; the C-terminal α-helix 19 is indicated. (B) Ribbon representation of the modeled N-ter domain of TCRV NP with bound RNA, rendered in black sticks. (C) (Left) Schematic of the asymmetric trimer model; the head-to-head interface between monomers A and B is indicated with a dashed circle. (Right) Predicted interface represented as ribbons. In panels A to C, relevant amino acid residues are shown as sticks. The color coding for NP is as in Fig. 1A.

overall impairment on their ability to support RNA synthesis (Fig. 3 and 4), which points to a critical role of NP-NP interaction mediated by residues L202, T205, D213, and L217 in assembly and/or activity of the RNP.

It has also been proposed that in the RNP, NP would arrange as a linear chain where the N-ter domain of one monomer would contact with the C-ter domain of a neighboring NP. Such an arrangement would be stabilized by head-to-tail contacts similar to those observed in the symmetric trimer (23). Specifically, LASV NP amino acids K56, Q190, D437, and D500 are presumed to participate in such head-to-tail interactions (21, 23). Evaluation of the role of homologous positions in TCRV NP (K56, Q185, D434, and D497) (Fig. 1C) showed that only those residues located at the N-ter domain (particularly Q185 and, to a lesser extent, K56) are important for NP self-association and nucleocapsid activity, while potential partners at the C-ter domain (D497 and D434) are not. These results might be explained by the existence of TCRV NP oligomeric forms different from the LASV NP symmetric trimer and/or by the TCRV NP multimeric arrangement being stabilized by NP-NP interactions other than the head-to-tail contacts predicted in the trimeric TCRV NP model.

Overall, the data reported here (summarized in Table 1) show a remarkable agreement between the NP N-terminal residues required for NP self-association and those essential for MG transcription and replication. Furthermore, the finding that amino

TABLE 1 Summary of representative NP variant phenotypes

NP type	NP-NP %[a]	FLUC %[b]	RNA binding %[c]	L binding[d]
WT	100	100	100	+
N-ter mutations				
Head				
D105A/K108A	−[e]	1	−	+
F287A/I288A	−	<1	−	+
Body				
K56A	35	43	90	+
L202A	3	4	−	+
D213A	−	<1	−	ND[f]
C-ter mutations				
G472A/R473A	96	<1	−	ND
D475A/L476A	90	<1	−	+
D497A	92	114	130	+

[a] Relative percentage of self-interaction, as determined in Fig. 2.
[b] Percentage of minigenome expression, as determined in Fig. 3.
[c] Estimated as the ratio of NP precipitated with RNA-agarose complexes to total NP in lysate, as reported in Fig. 6B.
[d] Mutations do not affect the interaction with the L polymerase, as reported in Fig. 5.
[e] −, undetectable.
[f] ND, not determined.

acids L202 and D213, located at the surface of NP and outside the RNA-binding crevice (Fig. 7B), are essential for binding to RNA strongly suggests that NP-NP interactions and binding of NP to RNA may be mutually cooperative.

Identification of C-terminal amino acids of NP essential for RNA binding and RNP activity. Recently, the structures of the C-terminal domain of TCRV NP (15) and JUNV NP (48) have been reported at resolutions of 1.8 and 2.2 Å, respectively. Superimposition with these crystal structures (PDB codes 4GVE and 4K7E, respectively) supported the overall validity of the TCRV NP model, confirming the correctness of the orientation predicted for the C-terminal residues analyzed, as well as its conservation in both NW arenavirus NPs (data not shown). The fact that both structures resemble that of the LASV NP C-terminal domain (15, 48) further supports the approach of modeling the full-length TCRV NP based on the structure of an OW arenavirus NP.

Residue D475 of TCRV NP and its flanking amino acids G472, R473, K474, and L476, as well as residues P452 and N453, located at a neighboring loop within the C-ter domain, were found to be dispensable for NP-NP interactions (Fig. 2). These results appear to be in contrast with the observation that residue D471 of LCMV NP (homologous to TCRV D475) is critically important for NP-NP interaction (40). This could be explained by taking into consideration the phylogenetic divergence between LCMV and TCRV, which raises the possibility that other residues at the C-ter domain of TCRV NP, not analyzed in this work, could be involved in NP self-association.

Interestingly, while substitution of C-terminal residue P452, N453, D434, or D497 had no impact, mutations G472A/R473A, K474A, and D475A/L476A caused a severe inhibition on FLUC activity through an overall effect on RNA synthesis (Fig. 3 to 4). Moreover, despite their wild-type capacities to self-associate, the G472A/R473A and D475A/L476A C-terminal mutants were found incompetent to bind RNA (Table 1). These results confirm that arenavirus RNA transcription and replication require the overall integrity of NP (11, 16). More importantly, our findings can also be interpreted to mean that the C-ter domain of NP, and specifically the D475-harboring loop, may contribute to viral RNA binding as well. Binding of RNA in a groove between the N- and C-terminal domains has been described for the nucleoprotein of other negative-strand RNA viruses, such as rabies virus, vesicular stomatitis virus (VSV), respiratory syncytial virus (RSV), and several members of the *Orthobunyavirus* genus (44–46, 49, 50). In addition, a similar configuration has been predicted for LASV NP (22). The loop comprising residues G472, R473, K474, D475, and L476, however, is located outside the region between the N-ter and C-ter domains of TCRV NP (Fig. 1A and D). A possibility is that substitutions at these positions may affect the overall domain folding, thus causing destabilization of the NP-RNA interaction. In any case, our data imply that binding of RNA mediated by the C-ter domain may occur independently of NP-NP interactions involving the N-ter domain. Further structural studies on OW and NW NP-RNA assemblies will be necessary to gain insight into the contribution of the C-ter domain of NP to RNA encapsidation.

In conclusion, three novel functional regions have been defined within TCRV NP in the present work (schematized in Fig. 8). Regions I and II comprise N-terminal residues critical for NP-NP interactions as well as for assembly of active RNP. The C-terminal region III harbors a structural element comprising residues essential for RNA binding. A possible interpretation of our results is that N-ter-to-N-ter (head-to-head) interactions may be involved in a transient RNA-free oligomeric configuration required for TCRV NP to polymerize on viral RNA. Additionally, NP-NP contacts mediated by the N-ter domain and RNA binding, mediated by both the N-ter and C-ter domains of NP, may cooperatively contribute to TCRV RNP assembly. In this scenario, side-by-side contacts between NP monomers, mediated by the N-ter domain, may also stabilize the nucleocapsid structure. In this regard, it is interesting to note that common structural features have been recognized in nucleocapsid-like particles from representative members of three negative-strand RNA virus families (*Rhabdoviridae*), *Paramyxoviridae* (genus *Pneumovirus*), and *Bunyaviridae* (genera *Phlebovirus* and *Orthobunyavirus*). These features include parallel orientation of nucleoprotein monomers in the linear nucleocapsid and extensive interactions among protein subunits, involving either one or both of the two (N-ter and C-ter) viral nucleoprotein domains (43).

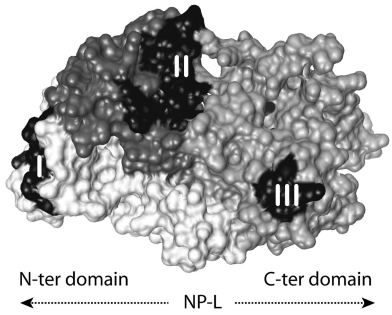

FIG 8 Surface representation of the TCRV NP monomer. Functional regions defined in this work are colored black. Region I, which is important for NP-NP interactions between monomers, comprises residues Q185 to L217. Region II, which is proposed to participate in RNA binding and in intramonomeric N-ter-to-C-ter contacts, includes α-helix 5 and residues G285 to I288. Region III, involved in RNA binding, includes residues G472 to L476. Color coding for other regions of NP is as in Fig. 1A. Binding to the L polymerase (NP-L) may involve multiple sites of interaction on both the N-ter and C-ter domains of NP.

Finally, it is broadly accepted that interaction of NP with the L polymerase must be important for viral RNP functionality. However, the L- and NP-interacting domain or domains remain unknown, and whether L interacts with monomeric or oligomeric forms of NP has not been defined. We found that NP mutants totally deficient for self-interaction (D105A/K108A, L202A, and F287A/I288A variants) are still capable of binding L (Table 1), suggesting that NP-NP association is not a requirement for the interaction between NP and the L polymerase and, therefore, that L may interact with NP monomeric forms. Moreover, analysis of NP deletion mutants indicated that both the N-ter and the C-ter domains are required for NP to bind L (Fig. 5B). Taken together, these results suggest that association with the L polymerase depends on multiple sites of interaction in both the N-ter and C-ter domains of TCRV NP. Although we cannot rule out that residues important for NP-NP association may be transiently engaged in weak interactions with the L polymerase, our results raise the possibility that NP-NP and NP-L binding functions may be structurally segregated on NP.

Due to the central role of NP in viral genome transcription and replication, identification of amino acid residues critically in-

volved in self-association and in interactions with the other RNP components gives insights into the viral nucleocapsid assembly process and may broaden the way toward the design of arenavirus-specific inhibitors.

ACKNOWLEDGMENTS

We are grateful to Gonzalo de Prat Gay (Fundación Instituto Leloir, Buenos Aires, Argentina) and Javier De Gaudenzi (Instituto de Investigaciones Biotecnológicas, Buenos Aires, Argentina) for helpful discussions and critical readings of the manuscript. We thank Markus Perbandt (University of Hamburg) for kindly providing us with the PDB coordinates of the LASV NP symmetric trimer structure. We also thank Martin A. Billeter (University of Zurich, Irchel, Switzerland) and Bernard Moss (National Institutes of Health, Bethesda, MD) for generously providing reagents. The technical assistance of J. Acevedo and S. Rojana is acknowledged.

This work was supported by Agencia Nacional de Promoción Científica y Tecnológica (ANPCyT) and CONICET. A.D., C.M.-B., and N.L. are research investigators of CONICET. S.F. receives a fellowship from ANPCyT (grant no. 1931/2008 to N.L.).

REFERENCES

1. **Charrel RN, de Lamballerie X, Emonet S.** 2008. Phylogeny of the genus Arenavirus. Curr. Opin. Microbiol. **11:**362–368. http://dx.doi.org/10.1016/j.mib.2008.06.001.
2. **Franze-Fernández MT, Iapalucci S, López N, Rossi C.** 1993. Subgenomic RNAs of Tacaribe virus, p 113–132. *In* Salvato MS (ed), The Arenaviridae. Plenum Press, New York, NY.
3. **Martínez-Peralta LA, Coto CE, Weissenbacher MC.** 1993. The Tacaribe complex: the close relationship between a pathogenic (Junin) and a non-pathogenic (Tacaribe) arenavirus, p 281–296. *In* Salvato MS (ed), The Arenaviridae. Plenum Press, New York, NY.
4. **Charrel RN, Coutard B, Baronti C, Canard B, Nougairede A, Frangeul A, Morin B, Jamal S, Schmidt CL, Hilgenfeld R, Klempa B, de Lamballerie X.** 2011. Arenaviruses and hantaviruses: from epidemiology and genomics to antivirals. Antiviral Res. **90:**102–114. http://dx.doi.org/10.1016/j.antiviral.2011.02.009.
5. **Buchmeier MJ, de la Torre JC, Peters CJ.** 2007. Arenaviridae: the viruses and their replication, p 1791–1828. *In* Knipe DM, Howley PM (ed), Fields virology, 5th ed, vol 2. Lippincott Williams & Wilkins, Philadelphia, PA.
6. **Hass M, Golnitz U, Muller S, Becker-Ziaja B, Günther S.** 2004. Replicon system for Lassa virus. J. Virol. **78:**13793–13803. http://dx.doi.org/10.1128/JVI.78.24.13793-13803.2004.
7. **Lee KJ, Novella IS, Teng MN, Oldstone MB, de la Torre JC.** 2000. NP and L proteins of lymphocytic choriomeningitis virus (LCMV) are sufficient for efficient transcription and replication of LCMV genomic RNA analogs. J. Virol. **74:**3470–3477. http://dx.doi.org/10.1128/JVI.74.8.3470-3477.2000.
8. **Lopez N, Jacamo R, Franze-Fernandez MT.** 2001. Transcription and RNA replication of Tacaribe virus genome and antigenome analogs require N and L proteins: Z protein is an inhibitor of these processes. J. Virol. **75:**12241–12251. http://dx.doi.org/10.1128/JVI.75.24.12241-12251.2001.
9. **Casabona JC, Levingston Macleod JM, Loureiro ME, Gomez GA, Lopez N.** 2009. The RING domain and the L79 residue of Z protein are involved in both the rescue of nucleocapsids and the incorporation of glycoproteins into infectious chimeric arenavirus-like particles. J. Virol. **83:**7029–7039. http://dx.doi.org/10.1128/JVI.00329-09.
10. **Groseth A, Wolff S, Strecker T, Hoenen T, Becker S.** 2010. Efficient budding of the Tacaribe virus matrix protein Z requires the nucleoprotein. J. Virol. **84:**3603–3611. http://dx.doi.org/10.1128/JVI.02429-09.
11. **Levingston Macleod JM, D'Antuono A, Loureiro ME, Casabona JC, Gomez GA, Lopez N.** 2011. Identification of two functional domains within the arenavirus nucleoprotein. J. Virol. **85:**2012–2023. http://dx.doi.org/10.1128/JVI.01875-10.
12. **Ortiz-Riano E, Cheng BY, de la Torre JC, Martinez-Sobrido L.** 2011. The C-terminal region of lymphocytic choriomeningitis virus nucleoprotein contains distinct and segregable functional domains involved in NP-Z interaction and counteraction of the type I interferon response. J. Virol. **85:**13038–13048. http://dx.doi.org/10.1128/JVI.05834-11.
13. **Shtanko O, Imai M, Goto H, Lukashevich IS, Neumann G, Watanabe T, Kawaoka Y.** 2010. A role for the C terminus of Mopeia virus nucleoprotein in its incorporation into Z protein-induced virus-like particles. J. Virol. **84:**5415–5422. http://dx.doi.org/10.1128/JVI.02417-09.
14. **Harmon B, Kozina C, Maar D, Carpenter TS, Branda CS, Negrete OA, Carson BD.** 2013. Identification of critical amino acids within the nucleoprotein of Tacaribe virus important for anti-interferon activity. J. Biol. Chem. **288:**8702–8711. http://dx.doi.org/10.1074/jbc.M112.444760.
15. **Jiang X, Huang Q, Wang W, Dong H, Ly H, Liang Y, Dong C.** 2013. Structures of arenaviral nucleoproteins with triphosphate dsRNA reveal a unique mechanism of immune suppression. J. Biol. Chem. **288:**16949–16959. http://dx.doi.org/10.1074/jbc.M112.420521.
16. **Martinez-Sobrido L, Emonet S, Giannakas P, Cubitt B, Garcia-Sastre A, de la Torre JC.** 2009. Identification of amino acid residues critical for the anti-interferon activity of the nucleoprotein of the prototypic arenavirus lymphocytic choriomeningitis virus. J. Virol. **83:**11330–11340. http://dx.doi.org/10.1128/JVI.00763-09.
17. **Martinez-Sobrido L, Giannakas P, Cubitt B, Garcia-Sastre A, de la Torre JC.** 2007. Differential inhibition of type I interferon induction by arenavirus nucleoproteins. J. Virol. **81:**12696–12703. http://dx.doi.org/10.1128/JVI.00882-07.
18. **Martinez-Sobrido L, Zuniga EI, Rosario D, Garcia-Sastre A, de la Torre JC.** 2006. Inhibition of the type I interferon response by the nucleoprotein of the prototypic arenavirus lymphocytic choriomeningitis virus. J. Virol. **80:**9192–9199. http://dx.doi.org/10.1128/JVI.00555-06.
19. **Zhou S, Cerny AM, Zacharia A, Fitzgerald KA, Kurt-Jones EA, Finberg RW.** 2010. Induction and inhibition of type I interferon responses by distinct components of lymphocytic choriomeningitis virus. J. Virol. **84:**9452–9462. http://dx.doi.org/10.1128/JVI.00155-10.
20. **Wolff S, Becker S, Groseth A.** 2013. Cleavage of the Junin virus nucleoprotein serves a decoy function to inhibit the induction of apoptosis during infection. J. Virol. **87:**224–233. http://dx.doi.org/10.1128/JVI.01929-12.
21. **Brunotte L, Kerber R, Shang W, Hauer F, Hass M, Gabriel M, Lelke M, Busch C, Stark H, Svergun DI, Betzel C, Perbandt M, Günther S.** 2011. Structure of the Lassa virus nucleoprotein revealed by X-ray crystallography, small-angle X-ray scattering, and electron microscopy. J. Biol. Chem. **286:**38748–38756. http://dx.doi.org/10.1074/jbc.M111.278838.
22. **Qi X, Lan S, Wang W, Schelde LM, Dong H, Wallat GD, Ly H, Liang Y, Dong C.** 2010. Cap binding and immune evasion revealed by Lassa nucleoprotein structure. Nature **468:**779–783. http://dx.doi.org/10.1038/nature09605.
23. **Hastie KM, Liu T, Li S, King LB, Ngo N, Zandonatti MA, Woods VL, Jr, de la Torre JC, Saphire EO.** 2011. Crystal structure of the Lassa virus nucleoprotein-RNA complex reveals a gating mechanism for RNA binding. Proc. Natl. Acad. Sci. U. S. A. **108:**19365–19370. http://dx.doi.org/10.1073/pnas.1108515108.
24. **Ortiz-Riano E, Cheng BY, de la Torre JC, Martinez-Sobrido L.** 2012. Self-association of lymphocytic choriomeningitis virus nucleoprotein is mediated by its N-terminal region and is not required for its anti-interferon function. J. Virol. **86:**3307–3317. http://dx.doi.org/10.1128/JVI.05503-11.
25. **Lennartz F, Hoenen T, Lehmann M, Groseth A, Garten W.** 2013. The role of oligomerization for the biological functions of the arenavirus nucleoprotein. Arch. Virol. **158:**1895–1905. http://dx.doi.org/10.1007/s00705-013-1684-9.
26. **Fuerst TR, Niles EG, Studier FW, Moss B.** 1986. Eukaryotic transient-expression system based on recombinant vaccinia virus that synthesizes bacteriophage T7 RNA polymerase. Proc. Natl. Acad. Sci. U. S. A. **83:**8122–8126. http://dx.doi.org/10.1073/pnas.83.21.8122.
27. **Radecke F, Spielhofer P, Schneider H, Kaelin K, Huber M, Dotsch C, Christiansen G, Billeter MA.** 1995. Rescue of measles viruses from cloned DNA. EMBO J. **14:**5773–5784.
28. **Jacamo R, Lopez N, Wilda M, Franze-Fernandez MT.** 2003. Tacaribe virus Z protein interacts with the L polymerase protein to inhibit viral RNA synthesis. J. Virol. **77:**10383–10393. http://dx.doi.org/10.1128/JVI.77.19.10383-10393.2003.
29. **Rossi C, Rey O, Jenik P, Franze-Fernandez MT.** 1996. Immunological identification of Tacaribe virus proteins. Res. Virol. **147:**203–211. http://dx.doi.org/10.1016/0923-2516(96)89650-6.
30. **Abramoff MD, Magalhaes PJ, Ram SJ.** 2004. Image processing with ImageJ. Biophotonics Int. **11:**36–42. http://webeye.ophth.uiowa.edu/dept/BIOGRAPH/ABRAMOFF/ImageJ.pdf.
31. **Caputi M, Mayeda A, Krainer AR, Zahler AM.** 1999. hnRNP A/B

proteins are required for inhibition of HIV-1 pre-mRNA splicing. EMBO J. **18:**4060–4067. http://dx.doi.org/10.1093/emboj/18.14.4060.

32. **Langland JO, Pettiford SM, Jacobs BL.** 1995. Nucleic acid affinity chromatography: preparation and characterization of double-stranded RNA agarose. Protein Expr. Purif. **6:**25–32. http://dx.doi.org/10.1006/prep.1995.1004.
33. **Di Tommaso P, Moretti S, Xenarios I, Orobitg M, Montanyola A, Chang JM, Taly JF, Notredame C.** 2011. T-Coffee: a web server for the multiple sequence alignment of protein and RNA sequences using structural information and homology extension. Nucleic Acids Res. **39:**W13–W17. http://dx.doi.org/10.1093/nar/gkr245.
34. **Eswa N, Webb B, Marti-Renom MA, Madhusudhan MS, Eramian D, Shen MY, Pieper U, Sali A.** 1 October 2006. Comparative protein structure modeling using Modeller. Curr. Protoc. Bioinformatics http://dx.doi.org/10.1002/0471250953.bi0506s15.
35. **Marti-Renom MA, Stuart AC, Fiser A, Sanchez R, Melo F, Sali A.** 2000. Comparative protein structure modeling of genes and genomes. Annu. Rev. Biophys. Biomol. Struct. **29:**291–325. http://dx.doi.org/10.1146/annurev.biophys.29.1.291.
36. **Wiederstein M, Sippl MJ.** 2007. ProSA-web: interactive web service for the recognition of errors in three-dimensional structures of proteins. Nucleic Acids Res. **35:**W407–W410. http://dx.doi.org/10.1093/nar/gkm290.
37. **Eisenberg D, Luthy R, Bowie JU.** 1997. VERIFY3D: assessment of protein models with three-dimensional profiles. Methods Enzymol. **277:**396–404. http://dx.doi.org/10.1016/S0076-6879(97)77022-8.
38. **Laskowski RA, Moss DS, Thornton JM.** 1993. Main-chain bond lengths and bond angles in protein structures. J. Mol. Biol. **231:**1049–1067. http://dx.doi.org/10.1006/jmbi.1993.1351.
39. **Maiti R, Van Domselaar GH, Zhang H, Wishart DS.** 2004. SuperPose: a simple server for sophisticated structural superposition. Nucleic Acids Res. **32:**W590–W594. http://dx.doi.org/10.1093/nar/gkh477.
40. **Ortiz-Riano E, Cheng BY, de la Torre JC, Martinez-Sobrido L.** 2012. D471G mutation in LCMV-NP affects its ability to self-associate and results in a dominant negative effect in viral RNA synthesis. Viruses **4:**2137–2161. http://dx.doi.org/10.3390/v4102137.
41. **Lopez N, Franze-Fernandez MT.** 2007. A single stem-loop structure in Tacaribe arenavirus intergenic region is essential for transcription termination but is not required for a correct initiation of transcription and replication. Virus Res. **124:**237–244. http://dx.doi.org/10.1016/j.virusres.2006.10.007.
42. **Kerber R, Rieger T, Busch C, Flatz L, Pinschewer DD, Kummerer BM, Günther S.** 2011. Cross-species analysis of the replication complex of Old World arenaviruses reveals two nucleoprotein sites involved in L protein function. J. Virol. **85:**12518–12528. http://dx.doi.org/10.1128/JVI.05091-11.
43. **Green TJ, Cox R, Tsao J, Rowse M, Qiu S, Luo M.** 2014. Common mechanism for RNA encapsidation by negative-strand RNA viruses. J. Virol. **88:**3766–3775. http://dx.doi.org/10.1128/JVI.03483-13.
44. **Niu F, Shaw N, Wang YE, Jiao L, Ding W, Li X, Zhu P, Upur H, Ouyang S, Cheng G, Liu ZJ.** 2013. Structure of the Leanyer orthobunyavirus nucleoprotein-RNA complex reveals unique architecture for RNA encapsidation. Proc. Natl. Acad. Sci. U. S. A. **110:**9054–9059. http://dx.doi.org/10.1073/pnas.1300035110.
45. **Ruigrok RW, Crepin T, Kolakofsky D.** 2011. Nucleoproteins and nucleocapsids of negative-strand RNA viruses. Curr. Opin. Microbiol. **14:**504–510. http://dx.doi.org/10.1016/j.mib.2011.07.011.
46. **Li B, Wang Q, Pan X, Fernandez de Castro I, Sun Y, Guo Y, Tao X, Risco C, Sui SF, Lou Z.** 2013. Bunyamwera virus possesses a distinct nucleocapsid protein to facilitate genome encapsidation. Proc. Natl. Acad. Sci. U. S. A. **110:**9048–9053. http://dx.doi.org/10.1073/pnas.1222552110.
47. **Ng AK, Lam MK, Zhang H, Liu J, Au SW, Chan PK, Wang J, Shaw PC.** 2012. Structural basis for RNA binding and homo-oligomer formation by influenza B virus nucleoprotein. J. Virol. **86:**6758–6767. http://dx.doi.org/10.1128/JVI.00073-12.
48. **Zhang Y, Li L, Liu X, Dong S, Wang W, Huo T, Guo Y, Rao Z, Yang C.** 2013. Crystal structure of Junin virus nucleoprotein. J. Gen. Virol. **94:**2175–2183. http://dx.doi.org/10.1099/vir.0.055053-0.
49. **Ariza A, Tanner SJ, Walter CT, Dent KC, Shepherd DA, Wu W, Matthews SV, Hiscox JA, Green TJ, Luo M, Elliott RM, Fooks AR, Ashcroft AE, Stonehouse NJ, Ranson NA, Barr JN, Edwards TA.** 2013. Nucleocapsid protein structures from orthobunyaviruses reveal insight into ribonucleoprotein architecture and RNA polymerization. Nucleic Acids Res. **41:**5912–5926. http://dx.doi.org/10.1093/nar/gkt268.
50. **Reguera J, Malet H, Weber F, Cusack S.** 2013. Structural basis for encapsidation of genomic RNA by La Crosse Orthobunyavirus nucleoprotein. Proc. Natl. Acad. Sci. U. S. A. **110:**7246–7251. http://dx.doi.org/10.1073/pnas.1302298110.